The Potential Energy Surface and Ro-Vibrational States of He−CH^+

Markus Meuwly*

Department of Chemistry, University of Durham, South Road, Durham, DH1 3LE, England

Nicholas J. Wright

The Fritz Haber Research Center for Molecular Dynamics, The Hebrew University, Jerusalem, 91904 Israel

Received: August 10, 1999; In Final Form: November 8, 1999

The potential energy surface (PES) for the interaction of He with CH^+ ($X^1\Sigma^+$) has been determined using *ab initio* CCSD(T) calculations. The resulting PES has a T-shaped minimum energy structure and a well depth of 477 cm^{-1}. Ro-vibrational calculations are performed to assess spectroscopic observables which should aid the experimental detection of this as yet unobserved system. Using an adiabatic correction scheme the influence of exciting the intermolecular (CH^+) stretching vibration is examined. For the electronic ground state no appreciable red shift of the monomer frequency is found in contrast to previously investigated systems of the same type. Exploratory calculations of the interaction between CH^+ ($a^3\Pi$) and He are presented in view of the ongoing interest in CH^+ in astrophysical environments. The $^3A''$ component has a deep T-shaped minimum energy structure with a well of about 900 cm^{-1}. Conversely, the $^3A'$ PES is comparatively isotropic with a linear geometry and a well of roughly 300 cm^{-1}.

I. Introduction

With the coupling of molecular beam and laser technology the structural and spectroscopic properties of an appreciable number of neutral Van der Waals molecules containing rare-gas atoms have been determined.[1,2] In parallel to these studies numerous theoretical investigations have been performed, leading to a detailed understanding of the interactions involved in binary systems.[3]

In contrast to neutral systems, studies involving ionic constituents are far less numerous. Recent reviews in this area include those of Castleman and Keesee,[4] Bieske and Maier,[5] and Castleman and Bowen.[6] In recent years, efforts to record high-resolution spectra of protonated ionic complexes have been undertaken in various groups. Following the pioneering microwave absorption work of Bogey and coworkers on Ar−H_3^+,[7,8] systems such as He−H^+_2,[9] Rg−OH^+,[10] Rg−HN_2^+,[1−13] Ar−CH_3^+,[14] and Rg−NH_4^+ [5] have been investigated (Rg = He, Ne, or Ar).

All systems mentioned above show profound differences when compared to neutral Van der Waals complexes. The potential energy surfaces (PESs) are often extremely anisotropic with relatively large interaction energies. Binding energies of the systems investigated so far vary between 300 cm^{-1} (He−HCO^+)[16] and as much as 6000 cm^{-1} (Ar−CH_3^+).[14] It has been found that the interaction energy between a rare gas atom and an ionic monomer AH^+ scales approximately linearly as a function of the difference between the proton affinities of the Rg atom B and the constituent A.[17]

The simplest systems for which accurate theoretical work can be undertaken are triatomic ionic complexes such as He−H_2^+,[18] He−HF^+,[19] and Rg−OH^+.[20] Another system in this series is He−CH^+. By pursuing a systematic characterization of the triatomic He−AH^+ systems it is hoped that an understanding which could be transferred to larger systems will be obtained. Apart from a straightforward continuation in a series of systems, He−CH^+ turns out to be a system of particular interest in its own right.

The CH^+ ion plays a central role in the chemistry of the interstellar medium. It was found, for example, in planetary nebulae and in translucent molecular clouds. One of the interests in CH^+ stems from its high abundance in diffuse interstellar clouds which is not easily explained.[21,22] As one possible precursor, CH^+ plays an important role in the carbon chemistry in diffuse clouds. Once formed, CH^+ is efficiently destroyed by reactions with H_2 to form CH_2^+ by way of which the carbon chemistry is initiated.[23] Given the sizeable amount of CH^+ and He available in molecular clouds, it might be interesting to investigate the interaction between the two constituents in some more detail. In addition, experiments in the mid-infrared might be equally possible, as already shown for various AH^+−B species.[11−13]

The aim of this work is to investigate the potential energy surface and bound states of the lowest electronic state of He−CH^+. Exploratory calculations relating to the first excited electronic state are presented as well. This is mainly because the $a^3\Pi$ state of CH^+ lies about 9000 cm^{-1} (which is in the astrophysically relevant 1 μm region) above the $X^1\Sigma$. Previous work on this system was performed by Hughes and von Nagy-Felsobuki[24] who reported the equilibrium geometry and the harmonic frequencies calculated at the CCSD(T) level of theory.

II. Theoretical Approach

All *ab initio* calculations were carried out with the Gaussian 94 program suite.[25] The basis set used consisted of Dunning's aug-cc-pVTZ basis set with the following contractions: C: (11s,6p,3d,2f) → [5s,4p,3d,2f]; He: (6s,3p,2d) → [4s,3p,2d]; H: (6s,3p,2d) → [4s,3p,2d].[26,27] The present work uses a Jacobi coordinate system, in which *R* describes the distance from the

* Corresponding author.

10.1021/jp9928107 CCC: $19.00
Published on Web 01/21/2000

TABLE 1: Comparison of Optimizations and Vibrational Frequencies of CH^+ and $He-CH^+$ Performed with Different Quantum Chemical Methods Using the aug-cc-pVTZ Basis Set[a]

method	state	r_{CH}/Å	r_{HHe}/Å	θ	ω_3/cm^{-1}	ω_2/cm^{-1}	ω_1/cm^{-1}	E_{tot} (E_h)
				CH^+				
MP2	$^1\Sigma^+$	1.1209					2932	−38.010630
MP2	$^3\Pi$	1.1199					2817	−37.980973
CCSD(T)	$^1\Sigma^+$	1.1288					2863	−38.024593
CCSD(T)	$^3\Pi$	1.1336					2704	−37.981386
				$He-CH^+$				
MP2	$^1A'$	1.1218	2.2699	81°	190	460	2956	−40.937513
CCSD(T)	$^1A'$	1.1292	2.2882	81°	190	432	2869	−40.976243
CCSD(T)[a]	$^1A'$	1.1290	2.2932	81°	189	427	2868	−40.977453
MP2	$^1A'$	1.1223	2.1741	0	−43	110	2953	−40.935994
CCSD(T)	$^1A'$	1.1302	2.1614	0	−57	114	2864	−40.974770
MP2	$^3A''$	1.1104	2.1876	101°	199	682	2940	−40.908827
CCSD(T)	$^3A''$	1.1211	2.1898	101°	214	666	2831	−40.934874
CCSD(T)[a]	$^3A''$	1.1210	2.1919	101°	204	671	2824	−40.935997
MP2	$^3A''$	1.1236	1.9111	0	125	154	2798	−40.906089
CCSD(T)	$^3A''$	1.1376	1.8701	0	125	158	2667	−40.932096

[a] The data in ref 24 were calculated using the CCSD(T) method and the slightly larger aug-cc-pCVTZ basis set. The linear transition states are reported as well.

center of mass of CH^+ to He. The angle θ is measured between the C-H axis and R, where $\theta = 0$ corresponds to a He−H−C geometry.

In a first step, optimized geometries at the MP2 and CCSD(T) level of theory are calculated. In these calculations all electrons are correlated. As can be seen from Table 1 the structures and harmonic frequencies are in reasonable agreement with previous work. In addition, it is observed that the CH^+ stretching vibration does not shift appreciably upon complex formation in the harmonic approximation. The small red shift is probably due to the "T-shaped" structure of the complex. The position and zero point motions of the He atom will be along a coordinate essentially orthogonal to the C-H stretching coordinate and therefore will have little effect upon it. This is in contrast to previously investigated systems[18−20] which have linear structures and therefore show much larger red shifts upon complexation.

The energy difference between the minimum energy structures of $He-CH^+$ $^1A'$ and $^3A''$ is about 9300 cm^{-1} at the CCSD(T) level. This compares with 9490 cm^{-1} for the free CH^+ ($3\Pi \leftarrow {}^1\Sigma$). (A previous CI calculation for the energy difference yielded 9230 cm^{-1}.[28]

A. Potential Energy Surface. The *ab initio* calculation of a potential energy surface requires the definition of a grid upon which the energies are calculated. The grid used in this work was chosen to facilitate close-coupling calculations of the bound states. Evaluation of the necessary integrals is stablest if Gauss-Legendre points are used for the angular coordinate θ. Therefore, calculations were performed at angles corresponding to an 8-point quadrature ($\theta = 16.20°, 37.19°, 58.29°, 79.43°, 100.57°, 121.70°, 142.81°$, and $163.80°$). In addition, the interaction potential was calculated in the two linear configurations ($\theta = 0$ and $\theta = 180°$).

For the ground state PES, the grid comprises 14 radial distances R between 3.2 a_0 and 15.0 a_0. These choices led to a good coverage of the PES which allows for an efficient and reliable interpolation of the *ab initio* points (*vide infra*). The CH^+ distance in the ground and excited electronic states was held fixed at the value resulting from geometry optimizations at the CCSD(T) level of theory (see Table 1). Keeping the CH^+ bondlength fixed at an equilibrium value can have an unpredictable effect upon the calculation, as has been shown for $He-OH^+$ and $Ne-OH^+$.[20] The influence of the C-H bond on the interaction potential will be investigated in more detail later on.

It is of some interest to consider the interaction between CH^+ in its first electronically excited state ($a^3\Pi$). Upon off-axis approach by a structureless partner, the intermolecular interaction will be described by two rather than one PES.[29] They are designated $^3A'$ and $^3A''$. It proved not advantageous to calculate interaction energies on an identical radial grid for each angle due to the rather large anisotropy in the case of the $^3A''$ surface. For $37.19° \leq \theta \leq 163.80°$, 23 values for R between 2.2 a_0 and 15.0 a_0 were chosen. For the remaining angles, the grid included 17 points between 3.0 a_0 and 15.0 a_0.

In order to ensure that a single-reference approach is valid, the $T1$ diagnostic has been calculated and was found to be sufficiently small.[30] Additionally, there is no nearby triplet state which could lead to large mixing.

Solving the Schrödinger equation for the motion of atomic nuclei on a PES requires the specification of the interaction between the constituents for arbitrary geometries. *Ab initio* calculations of interaction potentials are always carried out on a finite grid of selected points. Thus, a next step in the construction of a PES requires either an analytical fit of a parameterized functional form to the *ab initio* points or an interpolation between these points. The method chosen in this work is the Reproducing Kernel Hilbert Space interpolation scheme (RKHS).[31] It has proven to be a stable and efficient means to represent interaction energies, even on nonuniform grids.

The resulting PESs are displayed in Figure 1. They exhibit quite different overall behavior. The ground state surface has a primary well in a near T-shaped configuration with a well depth of −477 cm^{-1}. A second, very shallow minimum is present at the linear CH^+-He conformation. The fact that the linear geometry is only a faint local minimum is so far unique to any of the protonated AH^+-Rg complexes, where A is a base and Rg is a rare gas atom. All other similar systems investigated so far, such as $He-FH^+$, $He-OH^+$, $Ne-OH^+$, and $He-H_2^+$, show directional bonding along the AH^+-Rg axis and no T-shaped minima.[18−20]

The $^3A''$ PES describing He interacting with CH^+ in its electronically excited state has a much deeper well with an attraction energy of about −920 cm^{-1}. It is also in a near T-shaped configuration, and the minimum of the PES is closer to the C end of CH^+. The secondary minimum is deeper than for the ground state surface, which may result in more interesting dynamics associated with states close to the barrier separating

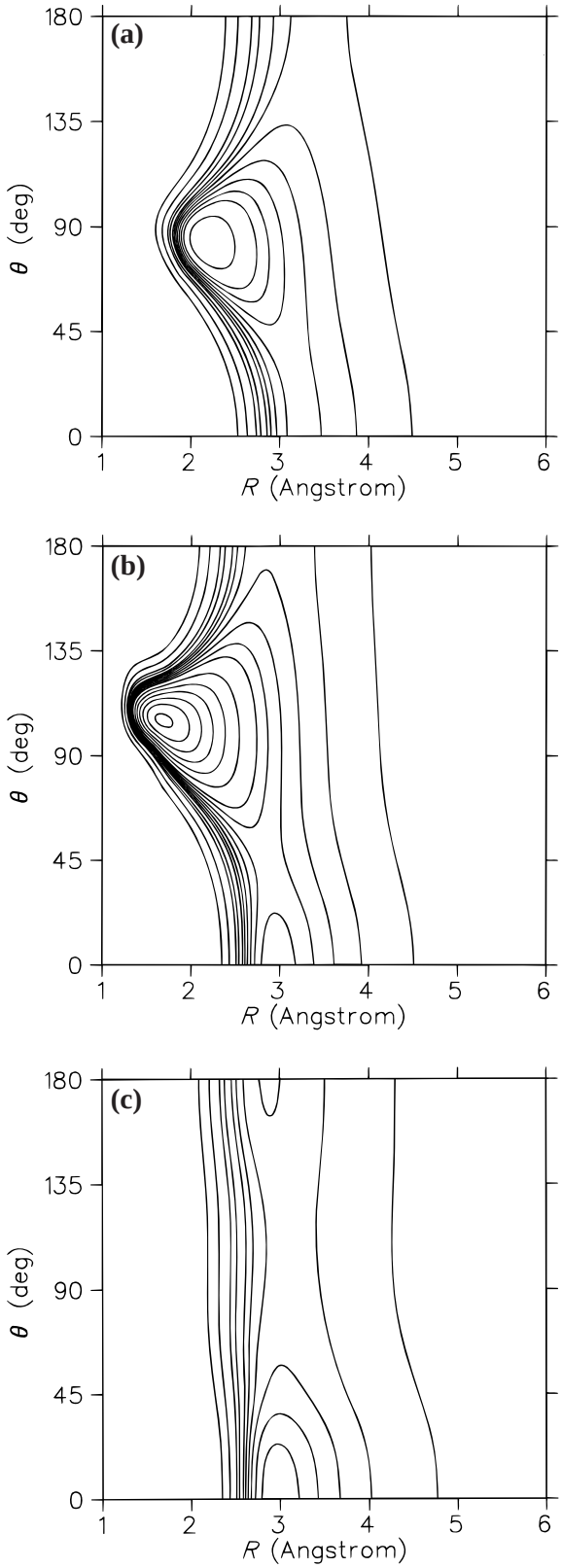

Figure 1. Plot of the potential energy surfaces for (a) He−CH$^+$ $^1A'$, (b) $^3A''$, and (c) $^3A'$. Contours on the repulsive wall are for 1000, 500, 200, and 100 cm^{-1}. Further contours between 0 and −250 cm^{-1} are drawn with a spacing of 50 cm^{-1}. Below −250 cm^{-1} the contours have a spacing of 100 cm^{-1}. For (a), the innermost contour is at −400 cm^{-1}, and for (b) it is at −900 cm^{-1}.

the two wells. This secondary minimum allows for a geometry optimization using conventional optimization techniques (see Table 1). Most prominent is the stronger repulsion in the excited state surface compared to the rather flat repulsive wall of the ground state potential.

TABLE 2: Stationary Points of the $^1A'$, $^3A''$, and $^3A'$ PESs for He−CH$^+$

electronic state	global minimum	local minimum	TS1	TS2
$^1A'$				
R_e (Å)	2.28	3.24	3.18	3.34
θ_e	83°	0	16°	180°
D_e (cm^{-1})	−477.1	−166.3	−165.0	−62.7
$^3A''$				
R_e (Å)	1.65	2.94	2.85	2.86
θ_e	106°	0	43°	180°
D_e (cm^{-1})	−918.5	−282.8	−221.5	−144.7
$^3A'$				
R_e (Å)	2.95	2.85	3.05	
θ_e	0	180°	111°	
D_e (cm^{-1})	−287.0	−155.3	−117.2	

In contrast to these two interaction potentials the $^3A'$ PES has a linear minimum energy configuration with a well depth of −287 cm^{-1}. The repulsive wall is shifted toward much larger intermolecular separations R and is considerably more isotropic. Compared to the interaction potentials for the $^1A'$ and the $^3A''$ state the potential minimum is less pronounced. It is of some interest to mention that the topology of the three PESs resemble quite closely those of the system Ar−BH which is not too suprising as BH is isoelectronic with CH$^+$.[32] The interaction energies, however, are much larger in the present case. The three PESs are displayed in Figure 1 and the stationary points characterizing them are summarized in Table 2.

III. Bound State Calculations

The states of He−CH$^+$ can be characterized by several quantum numbers: the CH stretching quantum number v_1, a bending quantum number v_2, which correlates in the isotropic limit with the CH$^+$ rotational quantum number j, the Van der Waals stretching quantum number v_3, the total angular momentum quantum number J, its projection K onto the molecule fixed z-axis, and the parity p. The only rigorously good quantum numbers for this system are J and p. Initially, $v_1 = 0$ as the *ab initio* calculations take no account of the variation of the potential with the C-H$^+$ distance. K is nearly conserved and, for the low lying states of He−CH$^+$, so are v_2 and v_3. For higher lying states, v_2 and v_3 are simply useful labels which qualitatively describe the wavefunction. A ro-vibrational state will therefore be characterized by a label (v_2v_3K). This notation has been previously used to describe ro-vibrational states in systems such as Ar−CO.[33]

The BOUND computer program[34] was used to perform close-coupling calculations of the ro-vibrational energy levels of He−CH$^+$. The He−CH$^+$ reduced mass is 3.06777161 m_u, and the rotational constants of the CH$^+$ monomer are 13.930 cm^{-1} for the $X^1\Sigma^+$ state and 13.747 cm^{-1} for the $a^3\Pi$ state.[35] In the basis set channels up to $j = 25$ have been included and the resulting coupled equations were solved using the log-derivative propagator.[36] The coupled equations are propagated from $R_{min} = 1.0$ Å to $R_{max} = 8.0$ Å, extrapolating to zero step size from log-derivative interval sizes of 0.01 Å and 0.02 Å using Richardson h^4 extrapolation. These parameters produce eigenvalues converged to better than 10^{-3} cm^{-1}.

IV. Results and Predictions

In the rigid rotor limit, He−CH$^+$ can be considered as an asymmetric rotor. But given the small difference in the B and C rotational constant from the *ab initio* calculations ($A = 431.96$

TABLE 3: Parameters for the Correction Function

	$v_1 = 0$			$v_1 = 1$		
	$f(0)$	a_1	a_2	$f(0)$	a_1	a_2
A/(cm^{-1})	-2.43×10^5	-2.43×10^5	5.4857	-6.98×10^5	-6.98×10^5	6.2279
C/(cm^{-1} Å^6)	-1.70×10^4	-1.70×10^4	13.9334	-5.14×10^4	-5.14×10^4	5.0165
	$v_1 = 0$			$v_1 = 1$		
	V_0	V_2	V_4	V_0	V_2	V_4
β/(Å^{-1})	3.1393	0.1018	0.0847	2.8916	0.1907	0.0017

GHz, $B = 35.51$ GHz, $C = 32.81$ GHz for He−CH$^+$($^1A'$) and $A = 464.58$ GHz, $B = 57.13$ GHz, $C = 50.87$ GHz for He−CH$^+$($^3A''$)), it is possible that the rotational analysis may be conveniently performed in terms of a prolate near-symmetric semirigid top framework.

The near-symmetric rotor energy level expression adopted is the one described by McKellar *et al.*[37]

$$E(J, K) = \bar{B}[J(J+1) - K^2] - D[J(J+1) - K^2]^2 + \Delta E_K$$

$$\Delta E_K = \pm\left(\frac{1}{4}(B - C)J(J+1) + \frac{1}{2}d[J(J+1)]^2\right) \qquad (1)$$

ΔE_K is zero for $K = 0$, both parameters in ΔE_K are allowed for $K = 1$, and only d is allowed for $K = 2$. In the actual fitting of the rotational lines it was not necessary to take d constants into account except for the (101) state of He−CH$^+$($^3A''$).

It is also customary to define *effective* rotational constants, *i.e.*, $\tilde{A}$, $\tilde{B}$, and $\tilde{C}$, which contain some centrifugal distortion contributions. In the following, the ro-vibrational energy levels are calculated using BOUND,[34] which performs a full dynamical calculation. The energy levels obtained include centrifugal distortion effects and any dynamical contributions. In comparing with possible experiments on He−CH$^+$, it is therefore convenient to define energy differences that may be qualitatively interpreted in terms of rigid-molecule rotational constants and prolate near-symmetric top centrifugal distortion constants. The appropriate expressions have been given by Thornley and Hutson[38] and are used to determine $\tilde{A}$, $\tilde{B}$, and $\tilde{C}$.

The resulting structural constants from both approaches can then be compared with expectation values $\langle 1/R^2 \rangle$ over the ro-vibrational wavefunction. This comparison helps to assess how reliable the underlying model Hamiltonian is.

A. $^1A'$ State. Close-coupling calculations on the He−CH$^+$ ($^1A'$) PES reveal that the ground state is 243 cm^{-1} below dissociation to He + CH$^+$ ($^1A'$). About half of the well depth is consumed by zero point energy. The average distance of the He atom to the center of mass of CH$^+$ is 2.40 Å, which is roughly 0.1 Å larger than the equilibrium separation.

Inspection of the expectation value $\langle 1/R^2 \rangle$ and wavefunction calculated in the helicity decoupled approximation reveal that the first excited $J = 0$ state is the Van der Waals stretch $v_3 = 1$ (010). It lies about 100 cm^{-1} higher in energy than the ground state. Due to the rather flat PES, this state already probes a much larger radial range than (000) as can be seen from the results collected in Table 4. However, the state is still concentrated around a T-shaped configuration as $\langle P_2 \rangle \approx -0.25$ suggests. The next fundamental (100) appears 167 cm^{-1} above (000) and is sensitive to a rather large part of the PES. The radial average is more than 3.0 Å, and the structure is far from T-shaped. In fact, the first bending state probes the whole angular range.

The $K = 1$ excitation of (100) is another 35 cm^{-1} higher in energy. This state has a node in the T-shaped configuration and a behavior similar to (100). Experiments able to characterize such states could obtain a lot of information on the topology of the underlying PES.

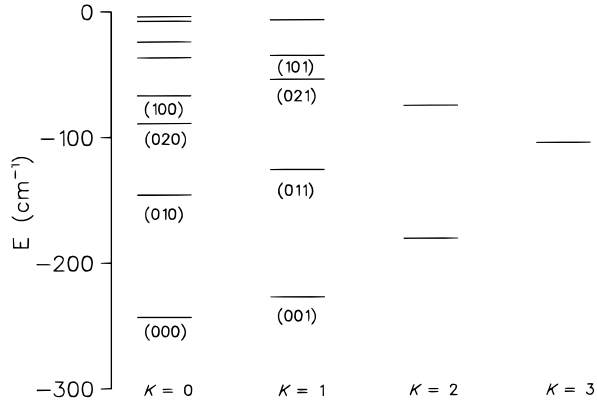

Figure 2. Bound states for He−CH$^+$ ($^1A'$). Only states with $J = K^+$ are shown.

TABLE 4: Energies and Expectation Values for the Ground State and the Lowest Excited Bending and Stretching States of He−CH$^+$ ($^1A'$) and ($^3A''$)

(v_2, v_3, K)	energy/cm^{-1}	ΔE/cm^{-1}	R_{av} = ($\langle 1/R^2 \rangle$)$^{-1/2}$/Å	$\langle P_2(\cos\theta) \rangle$
		CH$^+$ ($^1A'$)		
(000)	−243.47		2.40	−0.40
(010)	−145.88	97.5	2.68	−0.24
(100)	−66.92	167.5	3.07	−0.05
(101$^+$)	−35.31	208.2	3.02	−0.04
(101$^-$)	−35.36	208.1	2.93	−0.05
		CH$^+$ ($^3A''$)		
(000)	−528.52		1.88	−0.38
(010)	−373.42	155.10	1.98	−0.36
(100)	−178.30	350.22	2.41	−0.06
(101$^+$)	−153.49	375.03	2.33	−0.16
(101$^-$)	−153.53	374.99	2.33	−0.16

The vibrational energy levels of He−CH$^+$ ($^1A'$) are displayed in Figure 2. As can be seen the density of states is rather low. Progressions in K can be seen up to $K = 3$.

Rotational constants for the fundamentals were derived from levels up to $J = 5$. The methods described above to determine the rotational level pattern were used and lead to constants collected in Table 5. These structural constants can be compared with average distances derived from the wavefunctions for the corresponding vibrational levels themselves. Table 5 shows that for He−CH$^+$ ($^1A'$) the two forms of analysis described yield comparable results. In addition, rotational constants calculated from $\langle 1/R^2 \rangle$ compare to $\tilde{B}$ and $\bar{B}$ to within a few percent.

It is also of some interest to compare the frequencies calculated from the second derivatives around the minimum energy structure (see Table 1) with the bound states calculations. The presence of strong anharmonic effects combined with a substantial angular-radial coupling makes the calculation of frequencies based solely on information about the curvature around the minimum difficult.

TABLE 5: Rotational Constants Using Either a Prolate Near-Symmetric Rotor Hamiltonian or Effective Constants

	near-symmetric rotor				effective constants		
(υ_2, υ_3, K)	ν_0/cm^{-1}	$\bar{B}$/cm^{-1}	$D/10^{-4}$ cm^{-1}	$(B-C)$/cm^{-1}	$\tilde{A}$/cm^{-1}	$\tilde{B}$/cm^{-1}	$\tilde{C}$/cm^{-1}
			CH$^+$ ($^1A'$)				
(000)	−243.47	0.930	2.47		15.280	0.967	0.893
(010)	−145.88	0.751	3.78		19.479	0.786	0.715
(100)	−66.92	0.591	4.10		12.290	0.617	0.562
(001)	−228.10	0.931	2.36	0.073			
(011)	−126.28	0.771	3.17	0.070			
(101)	−54.70	0.632	4.01	0.054			
			CH$^+$ ($^3A''$)				
(000)	−528.52	1.484	4.98		15.304	1.565	1.401
(010)	−373.42	1.342	5.47		15.537	1.418	1.263
(100)	−178.30	0.948	8.76		23.838	0.927	0.965
(001)	−513.21	1.483	4.53	0.164			
(011)	−357.88	1.341	5.09	0.152			
(101)	−154.54	1.033	8.26	0.009			

B. Influence of the C-H$^+$ Coordinate. One customary and computationally useful approximation is to fix the monomer bond length at the equilibrium value of the geometry optimization for the complex. However, in the majority of protonated hydrogen-bonded systems it became obvious that monomers in different vibrational states interact differently with their binding partner. In order to include such effects a computationally efficient procedure was developed[39] and is implemented here to investigate how much the previous results are affected if the C-H$^+$ coordinate is considered.

The vibrational adiabatic procedure was applied in the form outlined in ref 16. The helium atom is placed at different intermolecular distances R_s along an angular cut specified by θ_c. In such a configuration the C-H bond is varied, which gives rise to an effective one-dimensional potential $V(r_{CH})$. The grid (R_s, θ_c) on which the correction function is calculated was chosen according to an energy criterion. The values of θ_c included 0, 45°, 60°, 90°, 120°, 135°, and 180°. On every angular cut R_s was determined as the solution of $V(R_s, \theta_c) = E_s$ where $E_s = 1000$ cm^{-1}, 0 cm^{-1}, $D_e(\theta_c)$ and $D_e(\theta_c)/2$. In addition, one point at $R_s = 10a_0$ was included for all angles.

For every position (R_s, θ_c) of the helium atom the C-H bondlength was varied between 1.5 a_0 and 2.75 a_0. Vibrational energies for the $\upsilon_1 = 0$ and $\upsilon_1 = 1$ vibrations were calculated using the LEVEL program.[40] The adiabatic correction for a specific R_s and θ_c is then defined as

$$V^{corr}(R_s, \theta_c; \upsilon) = E(R_s, \theta_c; \upsilon) - E(R_s, \theta_c = 180°; \upsilon) \quad (2)$$

Here, E is the energy of the $\upsilon_1 = 0$ or $\upsilon_1 = 1$ excitation.

Next, the correction potential $V^{adia}(R_s, \theta_c; \upsilon)$ is fitted to a functional form. Inspecting the radial behavior of each cut θ_c = constant reveals that $V^{adia}(R_s, \theta_c; \upsilon)$ is mainly repulsive. Thus, an exponentially decaying function augmented by a long-range attractive part is chosen:

$$V(R) = A\exp(-\beta R) - [\tanh(R - R_0) + 1]\frac{C}{R^6} \quad (3)$$

Although the long-range interaction of the physical potential is known to vary as R^{-4}, inspection of the correction potential did not seem to justify such a strong attraction at long range. The parameter R_0 is used to define the region in which the long-range contribution becomes important. It was fixed at $R_0 = 7.5$ a_0 in all cases.

Subsequently, the parameters A, β, and C are fitted to an angular-dependent expression. For A and C the expression

$$f(\theta) = f(0°) + a_1[e^{-a_2(1-\cos(\theta))} - 1] \quad (4)$$

was used. The parameter β was more appropriately represented by an expansion in Legendre polynomials of the form

$$\beta(\theta) = V_0 + V_2P_2(\cos\theta) + V_4P_4(\cos\theta) \quad (5)$$

The adiabatically corrected potentials are thus given by

$$V^{adia}(R, \theta; \upsilon) = V(R, \theta) - V^{corr}(R, \theta; \upsilon) \quad (6)$$

where $V(R, \theta)$ is the frozen monomer potential. The parameters for $\upsilon = 0$ and $\upsilon = 1$ are given in Table 3. It is interesting to note that the correction in the case of He−CH$^+$ does not significantly affect the well depth or the equilibrium structure. However, the repulsive wall is somewhat modified, especially in the He−H-C$^+$ configuration.

In order to fully assess the influence of the C-H$^+$ coordinate, ro-vibrational calculations on the $V^{adia}(R, \theta; \upsilon = 0)$ and $V^{adia}(R, \theta; \upsilon = 1)$ PESs have been performed. They confirm that only minor changes in the ro-vibrational states and the dissociation energy upon excitation of the C-H stretching vibration can be expected. The dissociation energy in the vibrational ground state is $D_0^{\upsilon_1=0} = -241$ cm^{-1} and decreases slightly to $D_0^{\upsilon_1=1} = -238$ cm^{-1} upon exciting the C-H stretch. Thus, no appreciable red-shift of the monomer vibration is expected as was observed in all previously studied AH$^+$−B complexes.[18−20] Harmonic frequencies calculated from the second derivatives around the minimum energy configuration (see Table 1) show the same behavior and support the present analysis.

The lower lying intermolecular stretching and bending excitations do not change in going from $\upsilon = 0$ to $\upsilon = 1$. They are also virtually unchanged compared to the results from calculations on the uncorrected PES. Thus, no in-depth analysis of these states has been performed. Once experimental data is available it may be advantageous to use the corrected PESs $V^{adia}(R, \theta; \upsilon = 0)$ and $V^{adia}(R, \theta; \upsilon = 1)$ together with the recently developed morphing procedure in order to devise improved interaction potentials.[41,42]

C. The Two Electronically Excited States $^3A'$ and $^3A''$. A complete treatment of the dynamics on the $^3A'$ and $^3A''$ PESs would have to include spin−orbit effects in calculating ro-vibrational energy levels. The main concern of the present work are the characteristics of the vibrational energy-level pattern, and as no experimental data is available the influence of such effects is neglected in the current study.

The far deeper well on the $^3A''$ surface compared to the ground state ($^1A'$) interaction potential leads to an increased binding energy. Again, the zero point energy consumes about half the well depth as emphasized by a binding energy of the (000) state of -530 cm^{-1}. This state has an average distance from the center of mass of CH^+ of 1.9 Å. The ground state probes largely a T-shaped configuration.

Some 160 cm^{-1} higher in energy lies the first excited stretching excitation (010). Due to the more confined topology of the PES, this state has an average radial distance only 0.1 Å larger than the ground state (000). This state is still concentrated around 90° as can be seen from plots of the wavefunction and averages over $\langle P_2 \rangle$. In contrast, the stretching excitation for He−CH^+ ($^1A'$) has an average separation about 0.3 Å larger than the ground state. As in He−CH^+ ($^1A'$) the first excited bending state is pushed up rather far, lying 350 cm^{-1} above the ground state and probing the whole angular range of the PES. Its $K = 1$ companion is found a further 25 cm^{-1} above.

Rotational constants for the lower lying states calculated from expectation values $\langle 1/R^2 \rangle$ agree far better with the effective constants than with the near-symmetric rotor analysis. This is not too surprising because the anisotropy of this interaction potential is rather large. However, as one moves up the ladder of vibrational excitations the two approaches should become very similar again, as was also observed in the electronic ground state. Indeed, for the (100) state (about 180 cm^{-1}) below dissociation, the rotational B constant calculated from $\langle 1/R^2 \rangle$ agrees with the value $\bar{B}$ from the near-symmetric rotor analysis.

The different topology of the PES for the $^3A'$ state leads to some profound changes in the ro-vibrational levels. Owing to its much reduced well depth, the lowest state is located just 135 cm^{-1} below dissociation to He + CH^+ ($^1\Pi$). Because the PES is rather flat, intermolecular stretching and bending vibrations are found at lower frequency than on the $^3A''$ potential. The (010) state is found 53 cm^{-1} above (000). Further fundamentals (101^+) and (100) lie 62 and 105 cm^{-1} above the ground state.

V. Conclusions

In contrast to all previously investigated protonated complexes between a linear monomer and a rare gas atom He−CH^+ shows a nearly T-shaped equilibrium structure in its electronic ground state. The PES has a pronounced well around $\theta = 90°$, and the ground state has large zero point energy contributions, consuming almost half of the well depth.

The system can be discussed using the approach pursued by Hutson.[43] Given the rather large anisotropy of the PES, it is not surprising that the energy level pattern has similarities with the case 3 coupling described in ref 43. In this coupling case the complex executes torsional oscillations about its equilibrium structure. However, this is the case only for the lowest states of He−CH^+($^1A'$). Rotational B-constants calculated from $\langle 1/R^2 \rangle$ are close to the ones resulting from the fit to a near-symmetric top. These values approach each other as the excitations in the Van der Waals bond increase. Thus, He−CH^+($^1A'$) can be appropriately described by a semirigid near-symmetric top Hamiltonian.

Given the more pronounced anisotropy of the He−CH^+ ($^3A''$) interaction one finds that more torsional states occur. Indeed, expanding the PES in terms of Legendre polynomials and evaluating V_2 for $R = R_e$ yields $(V_2/b) \approx 30$ and suggests that He−CH^+ ($^3A''$) may behave like a relatively rigid molecule for the lower bound states.

In contrast to the $^3A''$ state the $^3A'$ PES shows a linear minimum with a much reduced well depth. The interaction potential is flatter, and the repulsive wall is shifted towards larger intermolecular separations.

Experiments carried out in the mid-infrared region might probe the CH^+ stretching vibration of He−CH^+ in its electronic ground state and subsequently detect vibrationally predissociating CH^+ fragments. On the basis of the present investigation, no appreciable red shift of the CH^+ stretching frequency is expected. This is in contrast to observations in systems such as He−OH^+.[10,20] Additionally, the intermolecular excitations seem not to change considerably in going from He−CH^+ ($v_1 = 0$) to He−CH^+ ($v_1 = 1$). One of the bottlenecks to observe He−CH^+ may be that it proves difficult to produce enough CH^+ in a supersonic jet. But given the fact that He−CH^+ seems to behave differently than any other protonated complex observed to date and the possible astrophysical significance of this system it may be worthwhile taking this challenge.

The $^3A'' \leftarrow {}^1A'$ transition of He−CH^+ lies in a preferable region of the electromagnetic spectrum (1 μm) for ground based astrophysical investigations. However, the transition is likely to be only weakly allowed.[44] Nevertheless it may be worthwhile to investigate the dipole surface in some detail in order to have reliable estimates for transition strengths because both CH^+ and He might be sufficiently abundant to form He−CH^+ in interstellar environments.

Acknowledgment. M.M. acknowledges financial support from the Schweizerischer Nationalfonds zur Förderung der wissenschaftlichen Forschung. N.J.W. thanks the Royal Society for a postdoctoral fellowship. We thank Professor J. M. Hutson for help in implementing his BOUND program for this system. The calculations were partly carried out on a Silicon Graphics Origin 2000 computer system, which was purchased with funding from the Engineering and Physical Sciences Research Council. We thank Dr. Lydia Heck for her assistance in this context.

References and Notes

(1) Heaven, M. C. *J. Phys. Chem.* **1993**, *97*, 8567.
(2) Leopold, K. R.; Fraser, G. T.; Novick, S. E.; Klemperer, W. *Chem. Rev.* **1994**, *94*, 1845.
(3) Hutson, J. M. *Ann. Rev. Phys. Chem.* **1990**, *41*, 123.
(4) Castleman, A. W.; Keesee, R. G. *Chem. Rev.* **1986**, *86*, 589.
(5) Bieske, E. J.; Maier, J. P. *Chem. Rev.* **1993**, *93*, 2603.
(6) Castleman, A. W.; Bowen, K. *J. Phys. Chem.* **1996**, *100*, 12911.
(7) Bogey, M.; Bolvin, H.; Demuynck, C.; Destombes, J. L. *Phys. Rev. Lett.* **1987**, *58*, 988.
(8) Bogey, M.; Bolvin, H.; Demuynck, C.; Destombes, J. L.; Eijck, B. P. V. *J. Chem. Phys.* **1988**, *88*, 4120.
(9) Carrington, A.; Gammie, D. I.; Shaw, A. M.; Taylor, S. M.; Hutson, J. M. *Chem. Phys. Lett.* **1996**, *260*, 395.
(10) Roth, D.; Nizkorodov, S. A.; Maier, J. P.; Dopfer, O. *J. Chem. Phys.* **1998**, *109*, 3841.
(11) Meuwly, M.; Nizkorodov, S. A.; Maier, J. P.; Bieske, E. J. *J. Chem. Phys.* **1996**, *104*, 3876.
(12) Nizkorodov, S. A.; Meuwly, M.; Maier, J. P.; Dopfer, O.; Bieske, E. J. *J. Chem. Phys.* **1998**, *108*, 8964.
(13) Nizkorodov, S. A.; Spinelli, Y.; Bieske, E. J.; Maier, J. P.; Dopfer, O. *Chem. Phys. Lett.* **1997**, *265*, 303.
(14) Olkhov, R. V.; Nizkorodov, S. A.; Dopfer, O. *J. Chem. Phys.* **1998**, *108*, 10046.
(15) Dopfer, O.; Nizkorodov, S. A.; Meuwly, M.; Bieske, E. J.; Maier, J. P. *Int. J. Mass Spectrom.* **1997**, *167*, 637.
(16) Meuwly, M. *J. Chem. Phys.* **1999**, *110*, 4347.
(17) Nizkorodov, S. A.; Dopfer, O.; Meuwly, M.; Maier, J. P.; Bieske, E. J. *J. Chem. Phys.* **1996**, *105* (5), 1770.
(18) Meuwly, M.; Hutson, J. M. *J. Chem. Phys.* **1998**, *110*, 3418.
(19) Schmelz, T.; Rosmus, P. *Chem. Phys. Lett.* **1994**, *220*, 117.
(20) Meuwly, M.; Maier, J. P.; Rosmus, P. *J. Chem. Phys.* **1998**, *109*, 3850.

(21) Gredel, R. *Astron. Astrophys.* **1997**, *320*, 929.
(22) Dalgarno, A. *J. Chem. Soc., Faraday Trans.* **1993**, *89*, 2111.
(23) Millar, T. J.; Williams, D. A. *Rate Coefficients in Astrochemistry*; Kluver Academic Publishers: Dordrecht, Boston, London, 1988.
(24) Hughes, J. M.; von Nagy-Felsobuki, E. I. *Chem. Phys. Lett.* **1997**, *272*, 313.
(25) Frisch, M. J.; Trucks, G. W.; Schlegel, H. B.; Gill, P. M. W.; Johnson, B. G.; Robb, M. A.; Cheeseman, J. R.; Keith, T.; Petersson, G. A.; Montgomery, J. A.; Raghavachari, K.; Al-Laham, M. A.; Zakrzewski, V. G.; Ortiz, J. V.; Foresman, J. B.; Cioslowski, J.; Stefanov, B. B.; Nanayakkara, A.; Challacombe, M.; Peng, C. Y.; Ayala, P. Y.; Chen, W.; Wong, M. W.; Andres, J. L.; Replogle, E. S.; Gomperts, R.; Martin, R. L.; Fox, D. J.; Binkley, J. S.; Defrees, D. J.; Baker, J.; Stewart, J. P.; Head-Gordon, M.; Gonzalez, C.; Pople, J. A. *Gaussian 94*, Revision E.2; Gaussian, Inc.: Pittsburgh, PA, 1995.
(26) Dunning, T. H., Jr. *J. Chem. Phys.* **1989**, *90*, 1007.
(27) Woon, D.; Dunning, T., Jr. *J. Chem. Phys.* **1994**, *100*, 2975.
(28) Green, S.; Bagus, P. S.; Liu, B.; McLean, A. D.; Yoshimine, M. *Phys. Rev. A* **1972**, *5*, 1614.
(29) Alexander, M. H. *Chem. Phys.* **1985**, *92*, 337.
(30) Lee, T. J.; Rendell, A. P.; Taylor, P. R. *J. Phys. Chem.* **1990**, *94*, 5463.
(31) Ho, T. S.; Rabitz, H. *J. Chem. Phys.* **1996**, *104*, 2584.
(32) Alexander, M. H.; Gregurick, S.; Dagdigian, P. J. *J. Chem. Phys.* **1994**, *101*, 2887.
(33) Xu, Y.; McKellar, A. R. W. *Mol. Phys.* **1996**, *88*, 859.
(34) Hutson, J. M. *BOUND computer program*, version 5; distributed by Collaborative Computational Project No. 6 of the UK Engineering and Physical Sciences Research Council, 1993.
(35) Huber, K. P.; Herzberg, G. *Constants of Diatomic Molecules*; Van Nostrand: Princeton, 1962.
(36) Johnson, B. R. *J. Comput. Phys.* **1973**, *13*, 445.
(37) McKellar, A. R. W.; Zeng, Y. P.; Sharpe, S. W.; Wittig, C.; Beaudet, R. A. *J. Mol. Spectrosc.* **1992**, *153*, 475.
(38) Thornley, A. E.; Hutson, J. M. *Chem. Phys. Lett.* **1992**, *198*, 1.
(39) Meuwly, M.; Bemish, R. J. *J. Chem. Phys.* **1997**, *106*, 8672.
(40) Le Roy, R. J. Level computer program, University of Waterloo Chemical Physics Report cp-330, 1992.
(41) Meuwly, M.; Hutson, J. M. *J. Chem. Phys.* **1999**, *110*, 8338.
(42) Meuwly, M. *J. Chem. Phys.* **1999**, *111*, 2633.
(43) Hutson, J. M. *Adv. Mol. Vib. Chem. Coll. Dyn.* **1990**, *1*, 1.
(44) Carrington, A.; Softley, T. P. *Chem. Phys.* **1986**, *106*, 315.